

Optimal ISW detection and joint likelihood for cosmological parameter estimation

M. Frommert, T. A. Enßlin, & F. S. Kitaura

Max-Planck-Institut für Astrophysik, Karl-Schwarzschild-Straße 1, D-85748 Garching b. München, Germany
mona@mpa-garching.mpg.de

Accepted ????. Received ???; in original form July 2008

ABSTRACT

We analyse the local variance effect in the standard method for detecting the integrated Sachs-Wolfe effect (ISW) via cross-correlating the cosmic microwave background (CMB) with the large-scale structure (LSS). Local variance is defined as the systematic noise in the ISW detection that originates in the realisation of the matter distribution in the observed Universe. We show that the local variance contributes about 11 per cent to the total variance in the standard method, if a perfect and complete LSS survey up to $z \approx 2$ is assumed. Due to local variance, the estimated detection significance and cosmological parameter constraints in the standard method are biased. In this work, we present an optimal method of how to reduce the local variance effect in the ISW detection by working conditional on the LSS-data. The variance of the optimal method, and hence the signal-to-noise ratio, depends on the actual realisation of the matter distribution in the observed Universe. We show that for an ideal galaxy survey, the average signal-to-noise ratio is enhanced by about 7 per cent in the optimal method, as compared to the standard method. Furthermore, in the optimal method there is no need to estimate the covariance matrix by Monte Carlo simulations as in the standard method, which saves time and increases the accuracy. Finally, we derive the correct joint likelihood function for cosmological parameters given CMB- and LSS-data within the linear LSS formation regime, which includes a small coupling of the two datasets due to the ISW effect.

Key words: Cosmology: CMB – Large-Scale Structure – cosmological parameter estimation

1 INTRODUCTION

The integrated Sachs-Wolfe effect (ISW, Sachs & Wolfe (1967)) is an important probe of the existence and nature of dark energy (Crittenden & Turok 1996) and the nature of gravity (Lue et al. 2004; Zhang 2006b). Spatial curvature also gives rise to an ISW-effect, but is well constrained to be very close to zero by CMB-experiments such as WMAP (Komatsu et al. 2008). However, the detection of the ISW-signal remains challenging, for it is obscured by primordial fluctuations in the CMB. In recent years, substantial effort has been made to detect the integrated Sachs-Wolfe effect via cross-correlation of the CMB with large-scale-structure (LSS) surveys, such as optical galaxy and quasar surveys (SDSS, Adelman-McCarthy et al. (2008), and 2MASS, Jarrett et al. (2000)), radio surveys (NVSS, Condon et al. (1998)), and X-ray surveys (HEAO, Boldt (1987)). Such cross-correlation studies have e.g. been done by Boughn et al. (1998); Boughn & Crittenden (2004, 2005); Afshordi et al. (2004); Rassat et al. (2006); Raccanelli et al. (2008); McEwen et al. (2007); Pietrobon et al. (2006); Fosalba et al. (2003); Fosalba & Gaztañaga (2004); Vielva et al. (2006); Liu & Zhang (2006); Ho et al. (2008); and Giannantonio et al. (2008), just to name a few of them.

The standard method for detecting the cross-correlation between the large-scale structure and the CMB involves comparing the observed cross-correlation function with its theoretical prediction for a given fiducial cosmological model. The theoretical prediction is by construction an ensemble average over all possible realisations of the Universe given the fiducial parameters, including all possible realisations of the local matter distribution. Assuming ergodicity, this ensemble average can also be thought of as an average over all possible positions of the observer in the Universe ('cosmic mean').

However, the ISW effect is created by the decay of the gravitational potential coming from structures on the largest scales, i.e. from structures that have not yet undergone significant gravitational collapse and are still not decoupled from the expansion of the Universe. These largest scales are most affected by cosmic variance. Therefore, when comparing the observed (local) cross-correlation function to its cosmic mean value, the realisation of the matter distribution in our vicinity acts as a source of systematic noise in the estimation of the cross-correlation, hence leading to a biased detection significance, due to cosmic variance.

In this work, we estimate the contribution of this local variance effect to the total variance in the detected signal under the simpli-

fying assumption that there is no shot-noise in the galaxy distribution. We find that the local variance in the detected signal amounts to 11 per cent in the case of an ideal LSS survey going out to about redshift 2 and covering enough volume to include the large scales relevant for the ISW. This roughly agrees with Cabré et al. (2007), who compare different methods to estimate the error in standard cross-correlation studies. They find that their MC1 error, which ignores the variance coming from the realisation of the matter field and only considers the variance in the CMB-fluctuations, systematically underestimates the error by about 10 per cent.

From the above mentioned surveys, the local matter distribution is known to a certain degree, and hence the local variance effect can be reduced by working conditional on that information. We present a generic technique of how to include the knowledge of the matter distribution into the detection of the ISW via cross-correlation, hence reducing the sources of noise to the unknown part of the matter distribution and the primordial CMB-fluctuations. We define the systematic noise that comes from the known part of the matter distribution as bias, for it can be removed by working conditional on the LSS-data. Our method is referred to as optimal method, in contrast to the standard method for ISW detection mentioned above. The main idea of the optimal method is to create an ISW-template from a Wiener filter reconstruction of the large-scale structure. We then use this template to detect the amplitude of the ISW-template rather than of the theoretical cross-correlation function. This makes the variance in the estimated amplitude, and hence the signal-to-noise ratio depend on the actual realisation of the matter in the Universe. For an ideal LSS survey, we show that the average variance in the detected amplitude is reduced by 13 per cent in the optimal method. Rephrased in terms of the signal-to-noise ratio, this reduction of the noise leads on average to a higher detection significance by about 7 per cent. Furthermore, in the optimal method there is no need to estimate the covariance matrix by Monte Carlo simulations as in the standard method. This saves time and increases the accuracy of the method.

To our knowledge, the only methods for ISW detection suggested in the literature, besides this work, that also do not suffer from the local variance effect, are by Zhang (2006a) and Hernandez-Monteagudo (2008). The former involves combining lensing-LSS cross-correlation measurements with the ISW-LSS cross-correlation, and thereby relies on the nowadays still difficult lensing measurements (Hu 2001; Hu & Okamoto 2002). The latter follows an approach very similar to ours. However, Hernandez-Monteagudo (2008) does not use a Wiener filter reconstruction of the LSS distribution but works directly on the sphere. In contrast to our work he neglects the shot-noise, which could be easily included in his analysis, though. In this work we will go one step further than Hernandez-Monteagudo (2008) and derive the correct way of including the information encoded in the ISW for cosmological parameter estimation.

Many of the above mentioned cross-correlation studies have attempted to constrain cosmological parameters using a likelihood function for the cosmological parameters p given the observed cross-correlation function. Just like the detection significance, these parameter estimates are biased by local variance. Also, to our knowledge, there is no straightforward way of how to combine the likelihood function for the cross-correlation with the likelihoods for CMB- and LSS-data. In this work, we derive the correct joint likelihood function $P(T, \delta_g | p)$ for cosmological parameters, given the CMB-map T and the LSS-data δ_g , from first principles for the linear LSS formation regime. This joint likelihood consistently includes the coupling between the two datasets introduced by the

ISW effect, which so far has been neglected in analyses deriving cosmological parameter constraints by combining CMB- and LSS-data (Tegmark et al. 2004; Spergel et al. 2007).

The article is organized as follows. We start by briefly describing the integrated Sachs-Wolfe effect in section 2, and explain in detail the different stochastic processes that are relevant for our analysis in section 3. In section 4 we review the standard method for detecting the ISW via cross-correlation and estimate the contribution of the local variance to the total variance of the detected signal. Section 5 is devoted to presenting the optimal method of ISW-detection we developed, and to comparing it in detail to the standard method. We discuss the role of the biasing effect due to local variance in parameter constraints and derive the joint likelihood function $P(T, \delta_g | p)$ in section 6. Concluding remarks on our work are given in section 7.

2 THE INTEGRATED SACHS-WOLFE EFFECT

The effect of decaying gravitational potential fluctuations on the CMB is called the integrated Sachs-Wolfe effect and is described by

$$T_{\text{ISW}}(\hat{n}) = 2 \int_{\eta_{\text{ls}}}^{\eta_0} \Psi'(\eta, (\eta_0 - \eta) \hat{n}) d\eta, \quad (1)$$

where η denotes the conformal time, and η_{ls} and η_0 the conformal time at last scattering and today, respectively. Note that the integral in the above equation has to be taken along the backwards light-cone. Ψ is the gauge invariant Bardeen potential (Bardeen 1980), which coincides with the Newtonian gravitational potential in the Newtonian gauge used in this work. The prime denotes the derivative with respect to conformal time. In order to keep the notation simple we have redefined $T_{\text{ISW}} \equiv (T_{\text{ISW}} - T_0)/T_0$, where $T_0 = 2.725$ K is the temperature of the CMB-monopole. We will use this convention as well for T and T_{prim} , which will be defined in section 3.

In Newtonian gauge, T_{ISW} is obtained by applying a linear operator \mathcal{P} to the matter density contrast $\delta_m(\eta_0)$ today:

$$T_{\text{ISW}} = \mathcal{P} \delta_m(\eta_0). \quad (2)$$

The matter density contrast is defined as $\delta_m(x) \equiv (\rho_m(x) - \bar{\rho}_m)/\bar{\rho}_m$, where $\rho_m(x)$ denotes the density of matter in the Universe at position x , and $\bar{\rho}_m$ is the background matter density. Eq. (2) can be verified by using the perturbation equations derived by e.g. Kodama & Sasaki (1984) or Durrer (2001).

In order to obtain the expression for the operator \mathcal{P} in the subhorizon-limit, let us look at the Poisson equation

$$\Delta \Psi = \frac{3H_0^2}{2} (1+z) \Omega_m \delta_m, \quad (3)$$

where H_0 is the Hubble constant today, $\Omega_m \equiv \rho_{m,0}/\rho_{\text{crit},0}$ the ratio of matter density and critical density today, z denotes the redshift, and Δ is the Laplace operator in comoving coordinates. From the Poisson equation we obtain

$$\Psi'(k, \eta) = \frac{3H_0^2 \Omega_m}{2k^2} H(\eta) (1 - f(\eta)) G(\eta) \delta_m(k, \eta_0), \quad (4)$$

where $H(\eta)$ is the Hubble constant at conformal time η , $f \equiv d \ln \delta_m / d \ln a$ is the growth function, $G(\eta) \equiv \delta_m(k, \eta) / \delta_m(k, \eta_0)$ denotes the growth factor, and we define Fourier transformed quantities by

$$\delta_m(k, 0) = \int_V d^3x e^{ikx} \delta_m(x, 0). \quad (5)$$

The expression for the operator \mathcal{P} can then be obtained by Fourier transforming eq. (4) and inserting it into eq. (1). Note, though, that we have not used the subhorizon-limit in this work, for eq. (2) is valid on superhorizon-scales as well.¹

3 STOCHASTIC PROCESSES

3.1 Realisation of the matter distribution

In the standard cosmology adopted in this work, there are different stochastic processes to be considered. For simplifying the notation, let us define

$$G(x, C) \equiv \frac{1}{\sqrt{|2\pi C|}} \exp\left(-\frac{1}{2}x^\dagger C^{-1}x\right) \quad (6)$$

to denote a Gaussian probability distribution of the vector x around zero, given the cosmological parameters p and the covariance matrix $C \equiv \langle xx^\dagger \rangle$, where the averages are taken over the Gaussian distribution $G(x, C)$. Note that in general the covariance matrix depends on the cosmological parameters, which is not explicitly stated in our notation. A daggered vector or matrix denotes its transposed and complex conjugated version, as usual. Hence, given two vectors a and b , $a b^\dagger$ must be read as the tensor product, whereas $a^\dagger b$ denotes the scalar product. Note that these conventions can still be used for vectors and matrices in function-spaces, like e.g. the matter overdensity field δ_m , which is a continuous function of the position x .

During inflation, the matter density perturbations have been created from quantum fluctuations. This stochastic process was close to Gaussian (Mukhanov 2005), permitting to write down the probability distribution for the matter density contrast given the cosmological parameters p as

$$P(\delta_m | p) = G(\delta_m, S), \quad (7)$$

where the covariance matrix $S \equiv \langle \delta_m \delta_m^\dagger \rangle_{P(\delta_m | p)}$, depends on the cosmological parameters p . The average $\langle \dots \rangle_{P(\delta_m | p)}$ is defined as ensemble average over the different realisations of δ_m , the index $P(\delta_m | p)$ explicitly states which probability distribution the average has to be taken over. Given homogeneity and isotropy, we note that the Fourier transformation of S is diagonal

$$\langle \delta_m(k) \delta_m(k')^* \rangle_{P(\delta_m | p)} = (2\pi)^3 \delta(k - k') P(k), \quad (8)$$

where $P(k)$ is the power spectrum, $\delta(\dots)$ denotes the Dirac delta function, and the star is used for denoting complex conjugation.

¹ The correct formula for \mathcal{P} in Newtonian gauge, which also holds on superhorizon-scales, can be obtained by differentiating and Fourier transforming

$$\begin{aligned} \Psi(k, \eta) = & \exp\left(-\int_0^\eta p(k, \eta') d\eta'\right) \int_0^\eta \frac{4\pi G a^2 \rho_m}{3a'/a} \\ & \times G(k, \eta') \delta_m(k, \eta_0) \exp\left(\int_0^{\eta'} p(k, \eta'') d\eta''\right) d\eta' \end{aligned}$$

and inserting it into eq. (1), instead of the expression for $\Psi(k, \eta)$ in the subhorizon-limit, eq. (4). Here, we have defined $p(k, \eta) \equiv \frac{k^2 + 3a'^2/a^2}{3a'/a}$ and the linear growth factor $G(k, \eta) \equiv \frac{\delta(k, \eta)}{\delta(k, \eta_0)}$, which in general depends on the Fourier mode k .

The stochastic process due to the inflationary quantum fluctuations created the angular fluctuations in the CMB, that is, the primordial fluctuations originating from the surface of last scattering at redshift $z = 1100$, as well as the integrated Sachs-Wolfe effect imprinted by the more local matter distribution at $z < 2$. Throughout this work we will assume that the primordial fluctuations and the ISW are stochastically independent, which is a safe assumption (apart from the very large scales), given that they are associated with matter perturbations of very different wavelengths (Boughn et al. 1998), so that very little intrinsic cross-correlation can be expected. In fact, for notational convenience we will use the symbol δ_m to only denote the local matter distribution at $z < 2$. The joint probability distribution for $T_{\text{ISW}} = \mathcal{P}\delta_m$ and the primordial temperature fluctuations T_{prim} then factorises

$$P(T_{\text{ISW}}, T_{\text{prim}} | p) = P(T_{\text{ISW}} | p) P(T_{\text{prim}} | p), \quad (9)$$

with

$$P(T_{\text{ISW}} | p) = G(T_{\text{ISW}}, C_{\text{ISW}}), \quad (10)$$

and

$$P(T_{\text{prim}} | p) = G(T_{\text{prim}}, C_{\text{prim}}), \quad (11)$$

where we have defined the angular two-point auto-correlation function for the fluctuation T_X (X being 'ISW' or 'prim')

$$C_X \equiv \langle T_X T_X^\dagger \rangle_{P(T_X | p)}. \quad (12)$$

Again, given homogeneity and isotropy, C_X is diagonal in spherical harmonics space

$$\langle a_{lm}^X a_{l'm'}^{X*} \rangle_{P(T_X | p)} = C_l^X \delta_{ll'} \delta_{mm'}, \quad (13)$$

where C_l^X is the angular power spectrum of the quantity X , and we have used the expansion coefficients of T_X into spherical harmonics Y_{lm} ,

$$a_{lm}^X \equiv \int_S d\Omega T_X(\hat{n}) Y_{lm}^*(\hat{n}). \quad (14)$$

Given that the joint distribution $P(T_{\text{ISW}}, T_{\text{prim}} | p)$ factorises into two Gaussian distributions, the sum $T = T_{\text{ISW}} + T_{\text{prim}}$, which denotes the temperature fluctuation of the CMB, is again Gaussian distributed

$$P(T | p) = G(T, C_{\text{CMB}}), \quad (15)$$

with

$$C_{\text{CMB}} = C_{\text{ISW}} + C_{\text{prim}}. \quad (16)$$

Given the cosmological parameters, the angular power spectra C_l^{CMB} , C_l^{ISW} and C_l^{prim} can all be calculated using CMBFAST (<http://ascl.net/cmbfast.html>, Seljak & Zaldarriaga (1996)), CAMB (<http://camb.info>, Lewis et al. (2000)), or CMBEASY (www.cmbeasy.org, Doran (2005)). In particular, C_{ISW} can be obtained from the 3-dimensional matter covariance matrix S by

$$C_{\text{ISW}} = \mathcal{P} S \mathcal{P}^\dagger, \quad (17)$$

where we have used that linear transformations of Gaussian random variables are again Gaussian distributed, with the covariance matrix transformed accordingly, see also Cooray (2002).

3.2 CMB detector noise

From CMB-detectors, we do not read off the real T as defined in the last section, but a temperature where the detector noise T_{det}

has been added. Again this can be modeled as a Gaussian random process,

$$P(T_{\text{det}}) = G(T_{\text{det}}, C_{\text{det}}), \quad (18)$$

where C_{det} denotes the detector noise covariance. This process is independent of the process that created the real (noiseless) T , such that if we redefine $T \equiv T + T_{\text{det}}$ to be the temperature we read off our detector, we obtain

$$P(T|p) = G(T, C_{\text{CMB}} + C_{\text{det}}), \quad (19)$$

with C_{CMB} being the covariance matrix of the real (noiseless) CMB.

However, in most of this work we will neglect the detector noise, for the ISW is only present on the largest angular scales, where the dominant source of noise is cosmic variance (Afshordi 2004). The only part where we include the detector noise will be in section 6, where we derive the joint likelihood for the cosmological parameters, given CMB- and LSS-data, for in this likelihood we also include smaller angular scales.

3.3 Shot-noise

Unfortunately, the matter distribution is not directly known, and we have to rely on LSS catalogues from which we can try to reconstruct it. A process to be considered when working with such catalogues is the stochastic distribution of the galaxies, which only on average follows the matter distribution. Since the galaxies are discrete sources from which we want to infer the properties of the underlying matter overdensity field, we have to deal with shot-noise in the galaxy distribution. More specifically, we assume the observed number $N_g(x_i)$ of galaxies in a volume element $\Delta V(x_i)$ at a discrete position x_i to be distributed according to a Poisson distribution

$$P(N_g(x_i) | \lambda(x_i)) = \frac{\lambda(x_i)^{N_g(x_i)} e^{-\lambda(x_i)}}{N_g(x_i)!}. \quad (20)$$

Here, $\lambda(x)$ denotes the expected mean number of observed galaxies within $\Delta V(x)$, given the matter density contrast,

$$\lambda(x) = w(x) \bar{n}_g^r \Delta V (1 + b \delta_m(x)). \quad (21)$$

In the above equation, $\bar{n}_g^r \equiv N_g^{r, \text{tot}}/V$ denotes the cosmic mean galaxy density, with $N_g^{r, \text{tot}}$ being the total number of galaxies in the volume V . Note that we have added an index 'r' to stress that these are the actual (real) number of galaxies present in ΔV , as opposed to the observed number of galaxies N_g , which can be smaller due to observational detection limits. The window $w(x) \equiv \Phi(x) m(\hat{n})$ denotes the combined selection function $\Phi(x)$ and sky mask $m(\hat{n})$ of the survey, and b the galaxy bias, which in general depends on redshift, scale and galaxy type. The variance in the observed number of galaxies $N_g(x)$ within $\Delta V(x)$ is then $\sigma_g^2(x) \equiv \langle (N_g(x) - \lambda(x))^2 \rangle_{N_g} = \lambda(x)$. Here we have used the index N_g on the average to indicate the average over the Poisson distribution in eq. (20).

If the average number of galaxies $\lambda(x)$ is large, the Poisson distribution is well approximated by a Gaussian distribution around $\lambda(x)$. For simplicity we will use the Gaussian approximation throughout this work. Furthermore we will ignore the dependence of the noise on $\delta_m(x)$ by using $\sigma_g^2(x) = w(x) \bar{n}_g^r \Delta V$ instead of the correct noise term $\sigma_g^2(x) = \lambda(x)$, for the latter would require a non-linear and iterative approach. Such an approach is beyond the scope of this paper, but is also irrelevant for the main finding of this work. However, see Kitaura et al. (in preparation)

and Enßlin et al. (2008) for a better handling of the Poisson noise and bias variations.

Since the cosmic mean galaxy density \bar{n}_g^r is not known, we have to estimate it from the observed galaxy counts by

$$\bar{n}_g^r \Delta V \equiv \frac{N_g^{\text{tot}}}{\sum_{i=0}^{N_{\text{pix}}} w(x_i)}, \quad (22)$$

where N_g^{tot} is the total number of observed galaxies and the sum goes over all the pixels in our volume.

With the above mentioned simplifications, we can now work with the following linear data model. First we define the the observed galaxy density contrast at position x to be

$$\delta_g(x) \equiv \frac{N_g(x) - w(x) \bar{n}_g^r \Delta V}{\bar{n}_g^r \Delta V}. \quad (23)$$

We then write

$$\delta_g = R \delta_m + \epsilon, \quad (24)$$

where $\epsilon(x)$ is the additive noise-term that originates in the Poissonian distribution of $N_g(x)$, and $R(x_i, x_j) \equiv b w(x_i) \delta_{ij}$ is the linear response operator. Note that in general R maps the the continuous space in which δ_m lives onto the discrete pixel space of our data δ_g , and it can also include the mapping from redshift-space to comoving coordinate space. We have ignored both for the sake of notational simplicity. From the Poisson distribution in eq. (20), we see that $\langle \delta_g \rangle_{N_g} = R \delta_m$, and hence with the above simplifications the noise ϵ is Gaussian distributed around zero

$$P(\epsilon | p) = G(\epsilon, N), \quad (25)$$

with the noise covariance matrix

$$N(x_i, x_j) \equiv \langle \epsilon(x_i) \epsilon(x_j) \rangle_{N_g} = \frac{w(x_i)}{\bar{n}_g^r \Delta V} \delta_{ij}. \quad (26)$$

4 STANDARD CROSS-CORRELATION METHOD

4.1 Description

In this section we briefly review the standard method for detecting the cross-correlation of the CMB with the projected galaxy density contrast, which was first described by Boughn et al. (1998), but see for example also Ho et al. (2008) and Giannantonio et al. (2008)). Note that we use the word galaxy density contrast for convenience, but the method is of course the same when working with other tracers of the LSS as mentioned in section 1.

The theoretical cross-correlation function of two quantities $X(\hat{n})$ and $Y(\hat{n})$ on the sky is defined in spherical harmonics space as

$$C_l^{X,Y} \equiv \langle a_{lm}^X a_{lm}^{Y*} \rangle_{\text{all}}. \quad (27)$$

The average in the above definition is an ensemble average over all possible realisations of the Universe with given cosmological parameters, i.e. over $P(\delta_m, \delta_g, T | p)$. This is indicated by the index 'all' on the average. We will denote the abstract cross-correlation function as a vector in Hilbert space by $\xi^{X,Y}$ to simplify the notation. This can be understood as a vector in pixel space or as a vector in a_{lm} -space. Only when evaluating the expressions we derive, we will choose the representation of the abstract vector $\xi^{X,Y}$ in spherical harmonics space, $(\xi^{X,Y})_{lm'l'm'} = C_l^{X,Y} \delta_{ll'} \delta_{mm'}$. In the following we will work with the cross-correlation function of the projected galaxy density contrast with the CMB-temperature

fluctuations, $\xi^{g, \text{CMB}}$, in order to reproduce the standard approach in the literature.

The observed projected galaxy density contrast δ_g^{proj} in a given direction \hat{n} on the sky is

$$\delta_g^{\text{proj}}(\hat{n}) = \int dz \delta_g(x, z), \quad (28)$$

where δ_g is given by eq. (23). If the LSS survey and the CMB map cover the full sky, it is convenient to define an estimator for the cross-correlation function of the projected galaxy density contrast with the CMB in spherical harmonics space (Rassat et al. 2006),

$$\hat{C}_l^{g, \text{CMB}} \equiv \frac{1}{2l+1} \sum_m \text{Re}(a_{lm}^g a_{lm}^{\text{CMB}*}), \quad (29)$$

where a_{lm}^g and a_{lm}^{CMB} are the expansion coefficients of the observed δ_g^{proj} and T into spherical harmonics as defined in eq. (14). The hat has been added to discriminate the estimator of the cross-correlation function from its theoretical counterpart $C_l^{g, \text{CMB}}$. In the case that the experiments cover only a part of the sky, one has to take into account the effects of mode-coupling when working in spherical harmonics space. In this case it is therefore more straightforward to define other estimators for the cross-correlation function, such as averages over the sphere in real space (see e.g. Giannantonio et al. (2008)) or quadratic estimators as in Afshordi et al. (2004). However, for the statement we will make in this work the actual definition of the estimator is not relevant, and we find the one defined in spherical harmonics space the most convenient to work with, since a closely related quantity also appears within the framework of the optimal detection method presented later on in section 5. Again we use the abstract notation $\hat{\xi}^{g, \text{CMB}}$ for the estimator of the cross-correlation $\xi^{g, \text{CMB}}$.

In the literature, the probability distribution of the above defined estimator $\hat{\xi}^{g, \text{CMB}}$ around the theoretical cross-correlation function $\xi^{g, \text{CMB}}$ is usually approximated by a Gaussian,

$$P(\hat{\xi}^{g, \text{CMB}} | p) = G(\hat{\xi}^{g, \text{CMB}} - \xi^{g, \text{CMB}}, C), \quad (30)$$

where the covariance matrix of the cross-correlation estimator is defined as

$$C \equiv \langle (\hat{\xi}^{g, \text{CMB}} - \langle \hat{\xi}^{g, \text{CMB}} \rangle_{\text{all}}) (\hat{\xi}^{g, \text{CMB}} - \langle \hat{\xi}^{g, \text{CMB}} \rangle_{\text{all}})^\dagger \rangle_{\text{all}}. \quad (31)$$

The first question usually addressed in the above mentioned cross-correlation studies is whether a non-zero cross-correlation function can be detected at all. To this end one assumes a fiducial cosmological model (in this work we use the flat Λ CDM model with parameter values given by Komatsu et al. (2008), table 1: $\Omega_b h^2 = 0.02265$, $\Omega_\Lambda = 0.721$, $h = 0.701$, $n_s = 0.96$, $\tau = 0.084$, $\sigma_8 = 0.817$), which is used to predict the theoretical cross-correlation function and covariance matrix C . The latter is usually estimated by Monte Carlo simulations, see Cabré et al. (2007) for an overview, or analytically as in Afshordi et al. (2004). The analytical prediction is possible in the case that the joint probability distribution for the projected galaxy density contrast and CMB given the cosmological parameters, $P(\delta_g^{\text{proj}}, T_{\text{CMB}} | p)$, is Gaussian. Then the covariance matrix in spherical harmonics space can be expressed in terms of two-point correlation functions as

$$C_l = \frac{1}{(2l+1)f_{\text{sky}}} \left[(C_l^{g, \text{CMB}})^2 + C_l^g C_l^{\text{CMB}} \right], \quad (32)$$

where we have used the auto-correlation power-spectra for the projected galaxy density contrast and the CMB, which are defined as in

eq. (13). C_l^g contains by definition the power coming from the underlying matter distribution plus the shot-noise. Note that in principle, C_l^{CMB} in the above formula also includes detector noise, which we neglect here as discussed in section 3.2. f_{sky} is the fraction of the sky covered by both, the galaxy survey and the CMB experiment. In the following we will assume $f_{\text{sky}} = 1$.

Putting an amplitude or fudge factor A_{cc} in front of the theoretical cross-correlation function $\xi^{g, \text{CMB}}$ by hand, one can now find out whether it is possible to detect a non-zero A_{cc} . The index 'cc' on the amplitude indicates that it is the amplitude of the cross-correlation function. Of course this amplitude should be one in the fiducial model. However, even if the data are taken from a Universe in which the underlying cosmology is the fiducial model we will in general not estimate the amplitude to be one. This is due to the different sources of stochastic uncertainty or noise in the estimate of A_{cc} , which we have described at length in section 3. The likelihood for the amplitude given the cosmological parameters reads

$$P(\hat{\xi}^{g, \text{CMB}} | A_{cc}, p) = G(\hat{\xi}^{g, \text{CMB}} - A_{cc} \xi^{g, \text{CMB}}, C). \quad (33)$$

A commonly used estimator of the amplitude A_{cc} is the maximum likelihood amplitude

$$\begin{aligned} \hat{A}_{cc} &= \frac{\xi^{g, \text{CMB} \dagger} C^{-1} \hat{\xi}^{g, \text{CMB}}}{\xi^{g, \text{CMB} \dagger} C^{-1} \xi^{g, \text{CMB}}} \\ &= \frac{\sum_l (2l+1) \frac{C_l^{g, \text{CMB}} \hat{C}_l^{g, \text{CMB}}}{(C_l^{g, \text{CMB}})^2 + C_l^g C_l^{\text{CMB}}}}{\sum_l (2l+1) \frac{(C_l^{g, \text{CMB}})^2}{(C_l^{g, \text{CMB}})^2 + C_l^g C_l^{\text{CMB}}}}, \end{aligned} \quad (34)$$

where in the second line we have used the representation of the cross-correlation functions in spherical harmonics space and inserted eq. (32) for the covariance matrix C . The maximum likelihood amplitude is an unbiased estimator (if the underlying probability distribution is Gaussian), hence for the fiducial model we have for the average over all cosmic realisations

$$\langle \hat{A}_{cc} \rangle_{\text{all}} = 1, \quad (35)$$

since $\langle \hat{C}_l^{g, \text{CMB}} \rangle_{\text{all}} = C_l^{g, \text{CMB}}$ by definition of the latter quantity. Note that here we have assumed that the data are taken in a Universe where the underlying cosmology is actually the fiducial model. This will be assumed in the rest of the paper as well.

The variance in \hat{A}_{cc} is given by

$$\begin{aligned} \sigma_{cc}^2 &\equiv \langle (\hat{A}_{cc} - \langle \hat{A}_{cc} \rangle_{\text{all}})^2 \rangle_{\text{all}} \\ &= (\xi^{g, \text{CMB} \dagger} C^{-1} \xi^{g, \text{CMB}})^{-1} \\ &= \left[\sum_l (2l+1) \frac{(C_l^{g, \text{CMB}})^2}{(C_l^{g, \text{CMB}})^2 + C_l^g C_l^{\text{CMB}}} \right]^{-1}. \end{aligned} \quad (36)$$

In the standard literature, an estimated significance is given to the detection of the amplitude, the estimated signal-to-noise ratio

$$\left(\frac{\hat{S}}{N} \right)_{cc} \equiv \frac{\hat{A}_{cc}}{\sigma_{cc}} = \frac{\sum_l (2l+1) \frac{C_l^{g, \text{CMB}} \hat{C}_l^{g, \text{CMB}}}{(C_l^{g, \text{CMB}})^2 + C_l^g C_l^{\text{CMB}}}}{\sqrt{\sum_l (2l+1) \frac{(C_l^{g, \text{CMB}})^2}{(C_l^{g, \text{CMB}})^2 + C_l^g C_l^{\text{CMB}}}}}. \quad (37)$$

However, since the real signal is $A_{cc} = 1$, the actual signal-to-noise ratio is given by

$$\left(\frac{S}{N}\right)_{cc} \equiv \frac{1}{\sigma_{cc}} = \sqrt{\sum_l (2l+1) \frac{(C_l^{g,\text{CMB}})^2}{(C_l^{g,\text{CMB}})^2 + C_l^g C_l^{\text{CMB}}}}, \quad (38)$$

and is therefore independent of the data.

4.2 Analysis of error-contributions

In this section we analyse the different sources of noise that contribute to the total variance in eq. (36). In order to simplify this task we assume that there is no shot-noise in the galaxy distribution, that is, we set $\epsilon = 0$ in eq. (24), which means that the galaxies trace the matter distribution perfectly. Furthermore we work with the ideal case that we have a galaxy survey that covers the whole sky and goes out to redshift 2. With these two assumptions we have a perfect knowledge of the matter distribution δ_m relevant for the ISW.

The cross-correlation of the galaxy density contrast with the CMB is then effectively the cross-correlation of the ISW with the CMB, for T_{ISW} is obtained by applying a linear operator to δ_m as in eq. (2). We can therefore simply substitute all indices 'g' by the index 'ISW'. Furthermore we note that, since the ISW is uncorrelated with the primordial CMB-fluctuations, we have $C_l^{\text{ISW,CMB}} = C_l^{\text{ISW}}$. The index 'all' now indicates an average over the probability distribution $P(T_{\text{ISW}}, T_{\text{prim}} | p) = P(T_{\text{ISW}} | p)P(T_{\text{prim}} | p)$ (cf. section 3). Under the above assumptions, eq. (34) for the estimated amplitude reads

$$\hat{A}_{cc} = \frac{\sum_l (2l+1) \frac{\hat{C}_l^{\text{ISW,CMB}}}{C_l^{\text{ISW}} + C_l^{\text{CMB}}}}{\sum_l (2l+1) \frac{C_l^{\text{ISW}}}{C_l^{\text{ISW}} + C_l^{\text{CMB}}}}, \quad (39)$$

with the variance (eq. (36))

$$\sigma_{cc}^2 = \left(\sum_l (2l+1) \frac{C_l^{\text{ISW}}}{C_l^{\text{ISW}} + C_l^{\text{CMB}}} \right)^{-1}, \quad (40)$$

and the signal-to-noise ratio in eq. (38) simplifies to

$$\left(\frac{S}{N}\right)_{cc} = \sqrt{\sum_l (2l+1) \frac{C_l^{\text{ISW}}}{C_l^{\text{ISW}} + C_l^{\text{CMB}}}}. \quad (41)$$

The signal-to-noise ratio as a function of the maximum summation index l_{max} for our fiducial model is depicted in the top panel of Fig. 1, for which we have modified CMBEASY in order to obtain C_l^{ISW} and C_l^{CMB} . There are contributions to the signal-to-noise up to roughly $l = 100$. Note, though, that our assumptions of Gaussianity of the matter realisation δ_m and the assumption of \mathcal{P} being a linear operator do not hold on small scales where structure growth has become non-linear. However, this issue will not be addressed in this work and it will not affect our main results, which are due to advantages of our method on the very large scales, which are most affected by cosmic variance.

The above estimator for the amplitude is only unbiased when averaging over the joint distribution

$$\langle \hat{A}_{cc} \rangle_{\text{all}} \equiv \langle \langle \hat{A}_{cc} \rangle_{\text{prim}} \rangle_{\text{ISW}} = 1. \quad (42)$$

Here we indicate averages over $P(T_{\text{prim}} | p)$ and $P(T_{\text{ISW}} | p)$ by the indices 'prim' and 'ISW', respectively. This means that both, the primordial CMB-fluctuations and the realisation of the local matter distribution are part of the error budget. We call the latter the local variance, indicating that it originates in the realisation of the matter distribution in our observed Universe. Let us now estimate

the contribution of the local variance to the total variance of \hat{A}_{cc} . To this end we split the variance in eq. (36) into two parts

$$\begin{aligned} \sigma_{cc}^2 &\equiv \langle \langle (\hat{A}_{cc} - 1)^2 \rangle_{\text{prim}} \rangle_{\text{ISW}} \\ &= \langle \langle (\hat{A}_{cc} - \langle \hat{A}_{cc} \rangle_{\text{prim}})^2 \rangle_{\text{prim}} \rangle_{\text{ISW}} \\ &\quad + \langle \langle (\langle \hat{A}_{cc} \rangle_{\text{prim}} - 1)^2 \rangle_{\text{ISW}} \\ &\equiv \sigma_{\text{prim}}^2 + \sigma_{\text{loc}}^2, \end{aligned} \quad (43)$$

where we have defined the contributions to the variance coming from primordial CMB-fluctuations, and the local variance as σ_{prim}^2 and σ_{loc}^2 , respectively. Both can be easily calculated, and the second contribution turns out to be

$$\sigma_{\text{loc}}^2 = 2 \frac{\sum_l (2l+1) \frac{(C_l^{\text{ISW}})^2}{(C_l^{\text{CMB}} + C_l^{\text{ISW}})^2}}{\left(\sum_l (2l+1) \frac{C_l^{\text{ISW}}}{C_l^{\text{CMB}} + C_l^{\text{ISW}}} \right)^2}. \quad (44)$$

In the bottom panel of Fig. 1, we plot the relative contribution of the local to the total variance, $\sigma_{\text{loc}}^2 / \sigma_{cc}^2$ against the maximum l that we consider in the analysis, for our fiducial cosmological model. For a maximum multipole $l_{\text{max}} = 100$, this relative contribution amounts to

$$\frac{\sigma_{\text{loc}}^2}{\sigma_{cc}^2} \approx 11\%. \quad (45)$$

This estimate roughly agrees with Cabré et al. (2007), who compare different error estimates for the standard cross-correlation method. They compare what they call the MC1 method, which only takes into account the variance in the CMB and ignores the variance in the galaxy overdensity, with the MC2 method, which includes also the variance in the galaxy overdensity. Both methods rely on performing MC simulations of the CMB, and of the galaxy overdensity in the case of MC2, and the simulations used to compare the different error estimates have converged with an accuracy of about 5 per cent, as stated in the paper. The result is that, compared to the MC2 method, the MC1 method underestimates the error by about 10 per cent, which roughly agrees with our estimate.

5 OPTIMAL METHOD

Since the expected ISW-effect is known from our galaxy survey, it is possible to find a cross-correlation estimator that does not include the local variance in the error-budget, but is unbiased already when averaging conditional on the observed galaxy density contrast δ_g . We will introduce such an estimator in this section. To this end, we first derive the posterior distribution $P(T | \delta_g, p)$ for the CMB-temperature T , given the galaxy data δ_g and the cosmological parameters p . From that we obtain the maximum likelihood estimator for the amplitude of the part of T_{ISW} which is known from the galaxy survey. Since we assume everything to be Gaussian distributed, this maximum likelihood estimator is equivalent to the estimator we obtain from an optimal matched filter approach.

Note that a different attempt to make the detection of the ISW unbiased by the realisation of the local matter distribution was done by Zhang (2006a). It involves comparing CMB-galaxy and lensing-galaxy cross-correlation functions, and hence relies on nowadays still difficult lensing measurements.

Another work which does not suffer from local variance is by Hernandez-Montenegro (2008). He implements an optimal

matched filter in spherical harmonics space, and finds by numerical comparison that it always performs better than or equally well as the standard method. However, Hernandez-Monteagudo (2008) works directly on the sphere, without using a Wiener filter reconstruction of the LSS, and therefore is slightly suboptimal in exploiting the available 3-d information on galaxy positions.

In this work, we go one step further than Hernandez-Monteagudo (2008) and derive the joint likelihood for cosmological parameters, given CMB- and LSS-data, which includes the small coupling of the two datasets introduced by the ISW effect, cf. section 6.

5.1 Derivation of the posterior distribution

Let us first ask the question what the observed galaxy density contrast tells us about the matter distribution δ_m . Given the data model in eq. (24) and the noise distribution in eq. (25), we know that

$$\begin{aligned} P(\delta_g | \delta_m, p) &= P(\delta_g - R\delta_m | \delta_m, p) \\ &= G(\delta_g - R\delta_m, N). \end{aligned} \quad (46)$$

Using the probability distribution for δ_m given in eq. (7) as a prior for δ_m , we obtain the joint probability distribution $P(\delta_g, \delta_m | p) = P(\delta_g | \delta_m, p) P(\delta_m | p)$ of galaxies and matter distribution

$$\begin{aligned} P(\delta_g, \delta_m | p) &= G(\delta_g - R\delta_m, N) G(\delta_m, S) \\ &= G(\delta_m - Dj, D) G(\delta_g, RSR^\dagger + N), \end{aligned} \quad (47)$$

where we have defined the matter distribution uncertainty covariance matrix

$$D \equiv (R^\dagger N^{-1} R + S^{-1})^{-1} \quad (48)$$

and the response over noise weighted galaxy overdensity

$$j \equiv R^\dagger N^{-1} \delta_g, \quad (49)$$

which can be interpreted as the information source of our LSS-knowledge (Enßlin et al. 2008). A detailed derivation of the expression for the joint probability distribution in eq. (47) can be found in Appendix A. This distribution can be trivially integrated over δ_m in order to obtain the evidence

$$P(\delta_g | p) = G(\delta_g, RSR^\dagger + N). \quad (50)$$

Therefore the posterior distribution $P(\delta_m | \delta_g, p) = P(\delta_m, \delta_g | p) / P(\delta_g | p)$ reads

$$P(\delta_m | \delta_g, p) = G(\delta_m - Dj, D). \quad (51)$$

From this posterior one can directly read off the maximum a-posteriori estimator for the matter distribution δ_m

$$\delta_m^{\text{rec}} \equiv Dj = (R^\dagger N^{-1} R + S^{-1})^{-1} R^\dagger N^{-1} \delta_g. \quad (52)$$

This is the Wiener filter applied to the galaxy-overdensity (Wiener 1949; Zaroubi et al. 1995; Zaroubi 1995; Fisher et al. 1995; Erdoğan et al. 2004; Kitaura & Enßlin 2008). We call this estimator a *reconstruction* of the matter distribution from the galaxy survey, hence the symbol δ_m^{rec} .

With this knowledge of the matter distribution, let us now find the posterior distribution for $T = T_{\text{ISW}} + T_{\text{prim}} + T_{\text{det}}$, given the observed galaxy density contrast δ_g . The probability distribution for T_{ISW} , obtained from the one for δ_m , eq. (51), (note that we again use that linear transformations of Gaussian distributed random vectors are again Gaussian distributed, cf. eq. (17)), reads

$$P(T_{\text{ISW}} | \delta_g, p) = G(T_{\text{ISW}} - \tau, \mathcal{P}DP^\dagger), \quad (53)$$

where we have defined the ISW-template

$$\tau \equiv \mathcal{P} \delta_m^{\text{rec}}. \quad (54)$$

Since the uncertainty in the reconstructed matter distribution is not related to the primordial CMB-fluctuations (cf. section 3.1), the joint probability distribution for T_{ISW} , T_{prim} , and T_{det} given δ_g factorises:

$$\begin{aligned} P(T_{\text{ISW}}, T_{\text{prim}}, T_{\text{det}} | \delta_g, p) &= P(T_{\text{ISW}} | \delta_g, p) P(T_{\text{prim}} | p) \\ &\quad P(T_{\text{det}} | p). \end{aligned} \quad (55)$$

Note that in the above equation we have used the fact that the primordial CMB-fluctuations do not depend on the galaxy distribution. We now again use the fact that the sum of stochastically independent Gaussian distributed random variables is again Gaussian distributed with the sum of the covariance matrices. We then obtain the posterior distribution for T , given the LSS-data:

$$P(T | \delta_g, p) = G(T - \tau, \tilde{C}). \quad (56)$$

Here we have used the probability distribution for T_{prim} and T_{det} , eqs (11) and (18), and we have defined the covariance matrix for the total noise

$$\tilde{C} \equiv \mathcal{P}D\mathcal{P}^\dagger + C_{\text{prim}} + C_{\text{det}}. \quad (57)$$

As in section 4, we will neglect the detector noise in the rest of this section and only include it when deriving the likelihood in section 6. However, if needed it can easily be included into the following equations by replacing $C_{\text{prim}} \rightarrow C_{\text{prim}} + C_{\text{det}}$.

5.2 Estimation of the ISW amplitude

We can now ask the same question as before, namely if it is at all possible to detect a non-zero amplitude A_τ that we put in front of our ISW-template in eq. (56). Again we can write down the likelihood function for the amplitude

$$P(T | A_\tau, \delta_g, p) = G(T - A_\tau \tau, \tilde{C}), \quad (58)$$

and estimate the amplitude by a maximum likelihood estimator

$$\hat{A}_\tau = \frac{T_{\text{CMB}}^\dagger \tilde{C}^{-1} \tau}{\tau^\dagger \tilde{C}^{-1} \tau} = \frac{\sum_l (2l+1) \frac{\hat{C}_l^{\tau, \text{CMB}}}{\tilde{C}_l}}{\sum_l (2l+1) \frac{\hat{C}_l^\tau}{\tilde{C}_l}}, \quad (59)$$

where we have defined the estimator \hat{C}_l^τ of the ISW auto-correlation function analogous to the cross-correlation estimator in eq. (29):

$$\hat{C}_l^\tau \equiv \frac{1}{2l+1} \sum_m |a_{lm}^\tau|^2. \quad (60)$$

This maximum likelihood amplitude is again an unbiased estimator, but now with respect to the probability distribution conditional on δ_g ,

$$\langle \hat{A}_\tau \rangle_{\text{cond}} = 1, \quad (61)$$

where the index 'cond' on the average denotes an average over the distribution $P(T_{\text{CMB}} | A_\tau, \delta_g, p)$.

In other words, we have liberated ourselves from the part of the noise coming from the realisation of the part of δ_m that we know, hence reducing the sources of noise to the unknown part of δ_m and the primordial CMB-fluctuations. The variance in \hat{A}_τ is

$$\sigma_\tau^2 \equiv \langle (\hat{A}_\tau - \langle \hat{A}_\tau \rangle_{\text{cond}})^2 \rangle_{\text{cond}}$$

$$= \frac{1}{\tau^\dagger \tilde{C}^{-1} \tau} = \frac{1}{\sum_l (2l+1) \frac{\hat{C}_l^\tau}{C_l}}, \quad (62)$$

and we obtain the signal-to-noise ratio

$$\left(\frac{S}{N}\right)_\tau \equiv \frac{1}{\sigma_\tau} = \sqrt{\sum_l (2l+1) \frac{\hat{C}_l^\tau}{C_l}}. \quad (63)$$

Note that the error estimate (and hence the signal-to-noise ratio) of the optimal method depends on the concrete LSS realisation, and how well it is suited to detect the ISW effect. In a Universe, where by chance the local LSS does/does not permit a good ISW detection, the error is small/large, as it should be.

We would like to point out that in the optimal method there is no need to estimate the covariance matrices from Monte Carlo simulations, since for a given set of cosmological parameters, the matter covariance matrix (power spectrum) S can be calculated analytically using the fitting formula provided by Bardeen et al. (1986), since it is still linear on the scales we are interested in. C_{prim} can be obtained from Boltzmann codes such as CMBEASY, and the noise covariance N can be estimated from the data.

5.3 Comparison of signal-to-noise ratios and biasing

In order to compare our method to the standard one, let us now again make the simplifying assumption that there is no shot-noise in the galaxy distribution, and that we have a perfect galaxy survey, as we did in section 4.2. At the end of this section, we will also approximately look at the effects of a galaxy survey that is incomplete in redshift, i.e. that goes out to a maximal redshift $z_{\text{max}} < 2$. For the perfect survey, the shot-noise covariance matrix N is zero, and hence the posterior for δ_m in eq. (51) is infinitely sharply peaked around the reconstruction δ_m^{rec} (eq. (52)), which turns into

$$\begin{aligned} \delta_m^{\text{rec}} &= (R^\dagger N^{-1} R)^{-1} R^\dagger N^{-1} \delta_g \\ &= R^{-1} \delta_g. \end{aligned} \quad (64)$$

Here, R^{-1} should be read as the pseudo-inverse of R , e.g. as defined in terms of Singular Value Decomposition, see Press et al. (1992) and Zaroubi et al. (1995).

The posterior for δ_m in eq. (51) is therefore now a Dirac delta function

$$P(\delta_m | \delta_g, p) = \delta(\delta_m - R^{-1} \delta_g), \quad (65)$$

which makes our ISW-template exact, and the noise covariance matrix due to the error in the reconstruction is zero, $\mathcal{P}D\mathcal{P}^\dagger = 0$, hence leaving us with $\tilde{C} = C_{\text{prim}} = C_{\text{CMB}} - C_{\text{ISW}}$. Since our perfect LSS survey covers the complete volume relevant for the ISW, our template is now equal to the ISW-temperature fluctuations, $\tau = T_{\text{ISW}}$. We can then substitute all indices τ in eqs (59)-(63) by the index ISW, and the estimated amplitude becomes

$$\hat{A}_\tau = \frac{\sum_l (2l+1) \frac{\hat{C}_l^{\text{ISW,CMB}}}{C_l^{\text{CMB}} - C_l^{\text{ISW}}}}{\sum_l (2l+1) \frac{\hat{C}_l^{\text{ISW}}}{C_l^{\text{CMB}} - C_l^{\text{ISW}}}}, \quad (66)$$

with the variance

$$\sigma_\tau^2 = \left(\sum_l (2l+1) \frac{\hat{C}_l^{\text{ISW}}}{C_l^{\text{CMB}} - C_l^{\text{ISW}}} \right)^{-1}, \quad (67)$$

and the signal-to-noise ratio

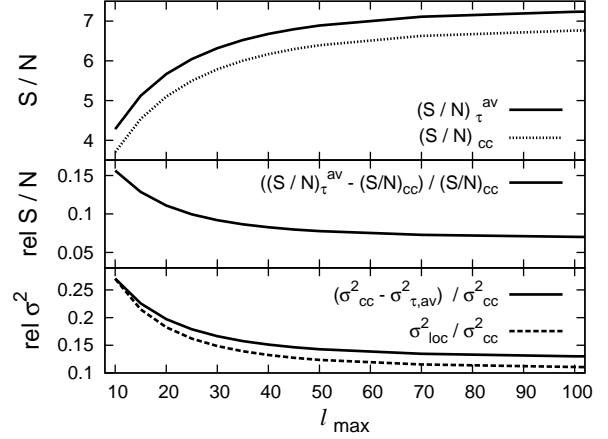


Figure 1. Comparison of the average signal-to-noise ratio and variance of the optimal method with the ones of the standard method for $z_{\text{max}} = 2$. Top panel: Average signal-to-noise ratio of the optimal method (solid) and signal-to-noise ratio of the standard method (dashed) versus the maximal multipole considered in the analysis. Middle panel: Relative improvement of the average signal-to-noise ratio in the optimal method. Bottom panel: Average relative improvement of the variance in the optimal method (solid) and relative contribution of the local variance to the total variance in the standard method (dashed)

$$\left(\frac{S}{N}\right)_\tau = \sqrt{\sum_l (2l+1) \frac{\hat{C}_l^{\text{ISW}}}{C_l^{\text{CMB}} - C_l^{\text{ISW}}}}. \quad (68)$$

As we mentioned before, the variance, and hence the signal-to-noise ratio of the optimal method, depend on the actual realisation of the matter distribution in our observed Universe. In Fig. 2, we plot the probability distribution of our signal-to-noise ratio for $l_{\text{max}} = 100$ and $z_{\text{max}} = 2$, which we have inferred from the distribution of T_{ISW} using the central limit theorem for $(S/N)_\tau^2$, and from that deriving the distribution for $(S/N)_\tau$. We have also checked the validity of the central limit theorem in this case by comparing with the correct probability distribution of the signal-to-noise ratio given by an expansion into Laguerre polynomials as derived e.g. in Castaño-Martínez & López-Blázquez (2007). The probability distribution is such that the signal-to-noise ratio can easily differ by $\Delta(S/N)_\tau \approx 1$ for two different realisations of the matter distribution.

The mean signal-to-noise ratio $(S/N)_\tau^{\text{av}} \equiv 1/\sqrt{\langle \sigma_\tau^2 \rangle} \equiv 1/\sqrt{\langle \sigma_\tau^2 \rangle_{\text{ISW}}}$ increases with l_{max} , as it did for the standard method. For every l_{max} we compare the mean signal-to-noise ratio of the optimal method to the signal-to-noise ratio of the standard method (cf. eq. (41)) in the top panel of Fig. 1, again for $z_{\text{max}} = 2$. Note that in our formula for the signal-to-noise ratio, eq. (68), there is now a minus sign between C_l^{CMB} and C_l^{ISW} , in contrast to the signal-to-noise ratio of the standard method in eq. (41), which has a plus sign instead. Thus we take advantage of the LSS instead of moving it into the error budget. The absolute enhancement of the signal-to-noise ratio in our method is therefore independent of l_{max} , for the main advantage of working conditional on the LSS arises on the very large scales, where the contribution of the ISW to the CMB is highest. The average relative improvement of the signal-to-noise is depicted in the middle panel of Fig. 1. It amounts to about 7 per cent for $l_{\text{max}} = 100$. In the bottom panel of Fig.

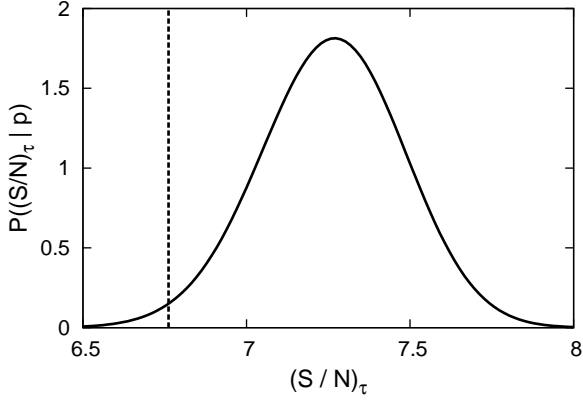


Figure 2. Probability distribution of the signal-to-noise ratio in the optimal method (solid) for $l_{\max} = 100$ and $z_{\max} = 2$. The vertical line (dashed) shows the signal-to-noise ratio of the standard method for comparison.

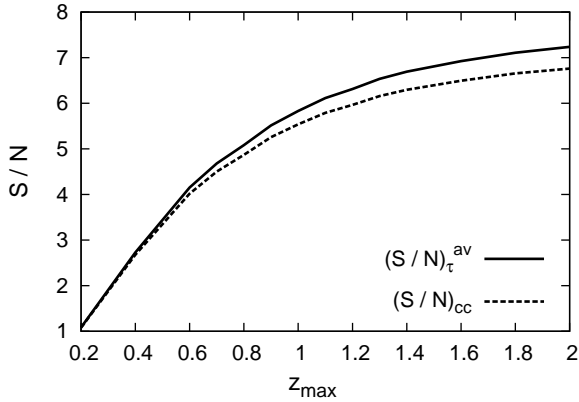


Figure 3. Average signal-to-noise ratio of the optimal method (solid) and signal-to-noise ratio of the standard method (dashed) versus z_{\max} for $l_{\max} = 100$.

1, we compare the mean relative improvement $(\sigma_{cc}^2 - \sigma_{\tau,av}^2)/\sigma_{cc}^2$ of the variance in the optimal method with the contribution of the local to the total variance in the standard method. The variance is reduced by about 13 per cent in the optimal method, as compared to the standard method.

Note that the maximal average signal-to-noise ratio we can hope for when trying to detect the ISW via cross-correlation, given a perfect LSS survey, is $(S/N)_{\tau}^{av} \approx 7.3$, with a variance as depicted in Fig. 2. Hence, if we are lucky and live in an environment that allows for a high signal-to-noise ratio, we can maximally obtain a detection significance of about $(7.5 - 8)\sigma$.

Let us now look at the effect of an incomplete galaxy survey. Incomplete galaxy surveys can be treated generically with our method, for the dark matter field, and hence the ISW effect, are split into a known part (the reconstruction) and an unknown part, which is an additive noise term, uncorrelated with the reconstruction. However, for now we only want to give a rough estimate of the consequences of an incomplete survey. Therefore we introduce a sharp cutoff in redshift, z_{\max} , and we simply redefine $T_{\text{ISW}} \equiv T_{\text{ISW}}(< z_{\max})$ to be the part of the ISW effect created at $z < z_{\max}$. The part of the ISW that has been created at $z > z_{\max}$ is then considered part of the primordial temperature

fluctuations T_{prim} . The power-spectra C_l^{ISW} and C_l^{prim} are redefined accordingly. With this redefinition we have introduced a correlation between what we consider the ISW and primordial fluctuations, which we would not have if we had used the reconstruction for redefining T_{ISW} . However, for getting the picture, we ignore this subtlety for the moment.

In Fig. 3, we plot the signal-to-noise ratio of the standard method together with the average signal-to-noise ratio of the optimal method versus z_{\max} for $l_{\max} = 100$, where we have used the above described redefinition of C_l^{ISW} in eqs (68) and (41). With decreasing maximal redshift of the LSS survey, the total signal-to-noise ratio in both methods goes down as does its relative enhancement of the optimal method as compared to the standard one. Also the relative contribution of the local to the total variance in the standard method goes down with decreasing survey depth.

As we stated in section 4.2, the amplitude-estimate of the standard method is biased when the averaging is performed conditional on the galaxy-data δ_g . This leads to an over- or underestimation of the detection significance, for the estimated amplitude is used when estimating the signal-to-noise ratio from the data. As we have shown, the contribution of the local to the total variance of the estimator is quite small, about 11 per cent for an ideal galaxy survey and even smaller for a shallower survey. However, we could be unlucky and live in an unlikely realisation of the matter distribution, given the power-spectrum, which would enhance the effect of the biasing.

With the method we presented in this work, the local variance effect is reduced. If we knew the local matter distribution perfectly, we would not be affected by local variance at all, as we have shown. Unfortunately, we have to rely on reconstructions of the matter distribution from LSS surveys, which suffer from shot-noise, and the effects of mask and selection function. However, the reconstruction treats mask and selection function in an optimal way, and extracts the maximum amount of information from the LSS data which can then be used in the ISW-detection.

6 LIKELIHOOD FUNCTION FOR COSMOLOGICAL PARAMETERS

The above described biasing effect is of course also present when moving on from the pure detection of the ISW to the task of constraining cosmological parameters using the ISW, which has been attempted in many of the above mentioned cross-correlation studies. This problem can already be seen in the likelihood function for the cosmological parameters of the standard method in eq. (30). The estimator of the cross-correlation function $\hat{\xi}_{g,\text{CMB}}$ could be quite different from the theoretical prediction with the underlying parameter values, just because we are living in an unlikely realisation of the matter distribution, given the power spectrum. Then the likelihood in eq. (30) would favour cosmological parameter values for which the theoretical prediction of the cross-correlation function is closer to its estimator, hence biasing the parameter estimates.

Furthermore, to our knowledge, there is no straightforward way of how to combine the likelihood from the cross-correlation in eq. (30) with the likelihoods for CMB- and LSS-data, as e.g. given in Verde et al. (2003), Percival et al. (2004) and Cole et al. (2005). Usually, when combining CMB- with LSS-data for deriving constraints on cosmological parameters, it is assumed that the two datasets are stochastically independent, i.e. that $P(T, \delta_g | p) = P(T | p) P(\delta_g | p)$, cf. Tegmark et al. (2004); Spergel et al. (2007); Komatsu et al. (2008). But the ISW effect (and also other effects as

e.g. the Sunyaev-Zel'dovich-effect) introduces a small stochastic dependence of the CMB-data on the LSS-data. That is, instead of assuming that the joint likelihood factorises, one should consider

$$P(T, \delta_g | p) = P(T | \delta_g, p) P(\delta_g | p), \quad (69)$$

in which we insert eq.s (56) and (50), obtaining

$$\begin{aligned} P(T, \delta_g | p) &= G(T - \tau, \tilde{C}) G(\delta_g, RSR^\dagger + N), \\ &= P(T | p) P(\delta_g | p) Q(T, \delta_g | p), \end{aligned} \quad (70)$$

and we recall for convenience the definition of \tilde{C} , eq. (57),

$$\tilde{C} \equiv \mathcal{P}D\mathcal{P}^\dagger + C_{\text{prim}} + C_{\text{det}},$$

of D , eq. (48),

$$D \equiv (R^\dagger N^{-1} R + S^{-1})^{-1},$$

and of τ , eq. (54),

$$\tau \equiv \mathcal{P}\delta_m^{\text{rec}}.$$

In the last step in eq. (70), we have expressed the joint likelihood in terms of the likelihoods $P(T | p)$ and $P(\delta_g | p)$ for only CMB- and only LSS-data, respectively, and the coupling term

$$\begin{aligned} Q(T, \delta_g | p) &\equiv \frac{P(T | \delta_g, p)}{P(T | p)} \\ &= \frac{G(T - \tau, \tilde{C})}{G(T, C_{\text{CMB}})}. \end{aligned}$$

Eq. (70) is the generic expression for the joint likelihood $P(T, \delta_g | p)$ for the cosmological parameters p , given CMB- and LSS-data, consistently including the small coupling term $Q(T, \delta_g | p)$ between the two datasets introduced by the ISW effect. The quantities depending on the cosmological parameters are S , C_{prim} , \mathcal{P} , R and, in general, N . Multiplying the likelihood by a prior $P(p)$ for the cosmological parameters, one can then sample the parameter space and derive constraints on the cosmological parameters from the posterior distribution $P(p | T, \delta_g) \propto P(T, \delta_g | p) P(p)$.

Note that this likelihood function remains valid if galaxy bias variations, position dependent noise, and other non-linear effects of galaxy formation are taken into account, as long as the variance of the reconstruction $D \equiv \langle (\delta_m^{\text{rec}} - \delta_m) (\delta_m^{\text{rec}} - \delta_m)^\dagger \rangle$ is estimated consistently (see Enßlin et al. (2008) for methods to treat such complications).

7 CONCLUSIONS

Due to the obscuration by primordial CMB-fluctuations, the detection of the integrated Sachs-Wolfe effect remains a challenge, and has to be performed by cross-correlating the CMB-signal with the large-scale structure. The standard method for doing so involves comparing the observed cross-correlation function to its theoretical prediction, which is by construction an ensemble average over all realisations of the primordial CMB-fluctuations and matter distributions. Hence, the realisation of the matter distribution in our Universe acts as a source of systematic noise in the estimate of the cross-correlation function, an effect that we have named the local variance.

Since the ISW is only present on the largest scales, the effect of the local variance is quite noticeable, amounting to about 11 per cent of the total variance in the standard method for an ideal LSS survey. This leads to a biased estimated detection significance

of the cross-correlation, and when moving on from the pure ISW-detection to parameter estimation, it also biases the parameter constraints. We note that even if the local variance contributes only about 11 per cent to the total variance of the detected signal, we could be unlucky and live in an unlikely realisation of the matter distribution, given the power-spectrum. This would enhance the effect of the bias on the detection significance and parameter constraints.

Given that information about the matter distribution can be inferred from the LSS survey, the local variance can be reduced by working conditional on this information. In this work, we have presented a generic technique of how to include the knowledge of the matter distribution into ISW detection in an optimal way, hence reducing the effect of the local variance. This optimal method requires a 3-d Wiener filter reconstruction of the LSS, including an estimator of the full reconstruction uncertainty covariance matrix. Note that also other reconstruction techniques that provide an estimator of the uncertainty covariance can easily be included into our method. The reduction of the local variance stresses the importance to measure and reconstruct the LSS to the highest possible accuracy, as aimed by Kitaura & Enßlin (2008) and Kitaura et al. (in preparation).

The conditionality on the LSS-data results in a dependence of the variance in the detected signal on the actual realisation of the matter distribution in the observed Universe. The average variance in the optimal method is reduced by about 13 per cent as compared to the standard method, again in the case of an ideal LSS survey. The reduction of the noise translates into an average enhancement of the signal-to-noise or detection significance by about 7 per cent for the optimal method. However, note that also the signal-to-noise ratio depends on the actual realisation of the matter distribution.

We would also like to point out that in the optimal method, there is no need to estimate the covariance matrix by Monte Carlo simulations, which saves time and increases the accuracy of the method (using 1000 Monte Carlo simulations to estimate the standard covariance matrix of the cross-correlation function only reaches an accuracy of about 5 per cent, as stated by Cabré et al. (2007)).

In order to consistently include the information encoded in the ISW effect for deriving cosmological parameter constraints, we have derived the joint likelihood $P(T, \delta_g | p)$ for the cosmological parameters p , given CMB- and LSS-data within the linear regime of structure formation. If one wishes to use the ISW effect for constraining cosmological parameters, one should include the additional CMB-galaxy data coupling term $Q(T, \delta_g | p)$, which we have factored out in eq. (70), into the usual likelihood analysis.

APPENDIX A: DERIVATION OF THE JOINT PROBABILITY DISTRIBUTION

In this section we will derive in detail the expression for the joint probability distribution $P(\delta_g, \delta_m | p)$ given in eq. (47). We start with

$$\begin{aligned} P(\delta_g, \delta_m | p) &= G(\delta_g - R\delta_m, N) G(\delta_m, S) \\ &= \frac{1}{\sqrt{|2\pi N| |2\pi S|}} \\ &\times \exp\left(-\frac{1}{2}(\delta_g - R\delta_m)^\dagger N^{-1}(\delta_g - R\delta_m)\right) \\ &\times \exp\left(-\frac{1}{2}\delta_m^\dagger S^{-1}\delta_m\right). \end{aligned} \quad (A1)$$

Let us first rewrite the exponent

$$\begin{aligned}
 & (\delta_g - R\delta_m)^\dagger N^{-1}(\delta_g - R\delta_m) + \delta_m^\dagger S^{-1}\delta_m \\
 &= \delta_m^\dagger D^{-1}\delta_m - 2j^\dagger \delta_m + \delta_g^\dagger N^{-1}\delta_g \\
 &= (\delta_m - Dj)^\dagger D^{-1}(\delta_m - Dj) - j^\dagger Dj + \delta_g^\dagger N^{-1}\delta_g \\
 &= (\delta_m - Dj)^\dagger D^{-1}(\delta_m - Dj) + \delta_g^\dagger (RSR^\dagger + N)^{-1}\delta_g, \quad (\text{A2})
 \end{aligned}$$

where we have used the definitions of D and j , eqs (48) and (49), in the first step, then completed the square in the second step, and we will separately prove the last step as Lemma 1 in the next subsection. After doing that we will prove that

$$|2\pi N||2\pi S| = |2\pi D||2\pi(RSR^\dagger + N)|, \quad (\text{A3})$$

which we name Lemma 2, allowing us to reformulate eq. (A1) as

$$\begin{aligned}
 &= \frac{1}{\sqrt{|2\pi D||2\pi(RSR^\dagger + N)|}} \\
 &\times \exp\left(-\frac{1}{2}(\delta_m - Dj)^\dagger D^{-1}(\delta_m - Dj)\right) \\
 &\times \exp\left(-\frac{1}{2}\delta_g^\dagger (RSR^\dagger + N)^{-1}\delta_g\right), \quad (\text{A4})
 \end{aligned}$$

which is what we claimed in eq. (47).

A1 Lemma 1

In this subsection we prove that

$$j^\dagger Dj - \delta_g^\dagger N^{-1}\delta_g = -\delta_g^\dagger (RSR^\dagger + N)^{-1}\delta_g. \quad (\text{A5})$$

In order to simplify the notation, let us introduce

$$M \equiv R^\dagger N^{-1}R. \quad (\text{A6})$$

It can be easily seen that eq. (A5) is equivalent to

$$N^{-1}R(S^{-1}+M)^{-1}R^\dagger N^{-1} - N^{-1} = -(RSR^\dagger + N)^{-1} \quad (\text{A7})$$

by inserting the respective expressions for D and j . We start with eq. (A7) and transform it into an equation which is true.

$$\begin{aligned}
 & N^{-1}R(S^{-1}+M)^{-1}R^\dagger N^{-1} - N^{-1} = -(RSR^\dagger + N)^{-1} \\
 \Leftrightarrow & N^{-1}RM^{-1}(M^{-1}+S)^{-1}SR^\dagger N^{-1} - N^{-1} \\
 &= -(RSR^\dagger + N)^{-1} \\
 \Leftrightarrow & (M^{-1}+S)^{-1}SR^\dagger N^{-1} - R^\dagger N^{-1} = -R^\dagger (RSR^\dagger + N)^{-1} \\
 \Leftrightarrow & SR^\dagger N^{-1} - (M^{-1}+S)R^\dagger N^{-1} \\
 &= -(M^{-1}+S)R^\dagger (RSR^\dagger + N)^{-1} \\
 \Leftrightarrow & -M^{-1}R^\dagger N^{-1} = -(M^{-1}+S)R^\dagger (RSR^\dagger + N)^{-1} \\
 \Leftrightarrow & M^{-1}R^\dagger N^{-1}(RSR^\dagger + N) = (M^{-1}+S)R^\dagger \\
 \Leftrightarrow & SR^\dagger + M^{-1}R^\dagger = (M^{-1}+S)R^\dagger \\
 \Leftrightarrow & (M^{-1}+S)R^\dagger = (M^{-1}+S)R^\dagger. \quad (\text{A8})
 \end{aligned}$$

This equation is true, q.e.d.

A2 Lemma 2

In the following we prove that

$$|2\pi N||2\pi S| = |2\pi D||2\pi(RSR^\dagger + N)|, \quad (\text{A9})$$

which is equivalent to

$$|N||S| = |D||RSR^\dagger + N|, \quad (\text{A10})$$

for the factors of 2π cancel for matrices that operate on the same vector space. Let us write

$$\begin{aligned}
 \frac{|N||S|}{|D|} &= |N||S||D^{-1}| \\
 &= |N||SD^{-1}| \\
 &= |N||S(S^{-1} + R^\dagger N^{-1}R)| \\
 &= |N| \exp(\log |1 + SR^\dagger N^{-1}R|) \\
 &= |N| \exp(\text{Tr} \log(1 + SR^\dagger N^{-1}R)) \\
 &= |N| \exp(\text{Tr} \log(1 + RSR^\dagger N^{-1})) \\
 &= |N| \exp(\log |1 + RSR^\dagger N^{-1}|) \\
 &= |N||RSR^\dagger N^{-1} + 1| \\
 &= |(RSR^\dagger N^{-1} + 1)N| \\
 &= |RSR^\dagger + N|. \quad (\text{A11})
 \end{aligned}$$

The crucial step here was to use the cyclic invariance of the trace Tr and to notice that this cyclic invariance still holds for the trace of a logarithm, which can be easily verified using the Taylor expansion of the logarithm.
q.e.d.

ACKNOWLEDGMENTS

The authors would like to thank Simon White, Thomas Riller, Carlos Hernandez-Monteagudo, Jens Jasche, Andre Waelkens, Tony Bandy, and Georg Robbers for useful discussions and comments.

REFERENCES

- Adelman-McCarthy J. K., Agüeros M. A., Allam S. S., et al. 2008, *ApJS*, 175, 297
 Afshordi N., 2004, *Phys. Rev. D*, 70, 083536
 Afshordi N., Loh Y.-S., Strauss M. A., 2004, *Phys. Rev. D*, 69, 083524
 Bardeen J. M., 1980, *Phys. Rev. D*, 22, 1882
 Bardeen J. M., Bond J. R., Kaiser N., Szalay A. S., 1986, *ApJ*, 304, 15
 Boldt E., 1987, *Phys. Rep.*, 146, 215
 Boughn S., Crittenden R., 2004, *Nature*, 427, 45
 Boughn S. P., Crittenden R. G., 2005, *New Astronomy Review*, 49, 75
 Boughn S. P., Crittenden R. G., Turok N. G., 1998, *New Astronomy*, 3, 275
 Cabré A., Fosalba P., Gaztañaga E., Manera M., 2007, *MNRAS*, 381, 1347
 Castaño-Martínez A., López-Blázquez F., 2007, *Test*, 14, 397
 Cole S., Percival W. J., Peacock J. A., et al. 2005, *MNRAS*, 362, 505
 Condon J. J., Cotton W. D., Greisen E. W., Yin Q. F., Perley R. A., Taylor G. B., Broderick J. J., 1998, *AJ*, 115, 1693
 Cooray A., 2002, *Phys. Rev. D*, 65, 103510
 Crittenden R. G., Turok N., 1996, *Physical Review Letters*, 76, 575
 Doran M., 2005, *Journal of Cosmology and Astro-Particle Physics*, 10, 11
 Durrer R., 2001, *astro-ph/0109522*
 Enßlin T. A., Frommert M., Kitaura F. S., 2008, submitted, *astro-ph/0806.3474*

- Erdođdu P., Lahav O., Zaroubi S., et al. 2004, MNRAS, 352, 939
- Fisher K. B., Lahav O., Hoffman Y., Lynden-Bell D., Zaroubi S., 1995, MNRAS, 272, 885
- Fosalba P., Gaztañaga E., 2004, MNRAS, 350, L37
- Fosalba P., Gaztañaga E., Castander F. J., 2003, ApJ, 597, L89
- Giannantonio T., Scranton R., Crittenden R. G., Nichol R. C., Boughn S. P., Myers A. D., Richards G. T., 2008, astro-ph/0801.4380
- Hernandez-Monteagudo C., 2008, submitted, astro-ph/0805.3710
- Ho S., Hirata C. M., Padmanabhan N., Seljak U., Bahcall N., 2008, astro-ph/0801.0642
- Hu W., 2001, ApJ, 557, L79
- Hu W., Okamoto T., 2002, ApJ, 574, 566
- Jarrett T. H., Chester T., Cutri R., Schneider S., Skrutskie M., Huchra J. P., 2000, AJ, 119, 2498
- Kitaura F. S., Enßlin T. A., 2008, MNRAS in press, astro-ph/0705.0429
- Kodama H., Sasaki M., 1984, Progress of Theoretical Physics Supplement, 78, 1
- Komatsu E., Dunkley J., Nolte M. R., et al. 2008, astro-ph/0803.0547
- Lewis A., Challinor A., Lasenby A., 2000, ApJ, 538, 473
- Liu X., Zhang S.-N., 2006, ApJ, 636, L1
- Lue A., Scoccimarro R., Starkman G., 2004, Phys. Rev. D, 69, 044005
- McEwen J. D., Vielva P., Hobson M. P., Martínez-González E., Lasenby A. N., 2007, MNRAS, 376, 1211
- Mukhanov V., 2005, Physical foundations of cosmology. Physical foundations of cosmology, by V. Mukhanov. Cambridge, UK: Cambridge University Press, 2005
- Percival W. J., Burkey D., Heavens A., et al. 2004, MNRAS, 353, 1201
- Pietrobon D., Balbi A., Marinucci D., 2006, Phys. Rev. D, 74, 043524
- Press W. H., Teukolsky S. A., Vetterling W. T., Flannery B. P., 1992, Numerical recipes in C. The art of scientific computing. Cambridge: University Press, —c1992, 2nd ed.
- Raccanelli A., Bonaldi A., Negrello M., Matarrese S., Tormen G., de Zotti G., 2008, MNRAS, 386, 2161
- Rassat A., Land K., Lahav O., Abdalla F. B., 2006, astro-ph/0610911
- Sachs R. K., Wolfe A. M., 1967, ApJ, 147, 73
- Seljak U., Zaldarriaga M., 1996, ApJ, 469, 437
- Spergel D. N., Bean R., Doré O., et al. 2007, ApJS, 170, 377
- Tegmark M., Strauss M. A., Blanton M. R., et al. 2004, Phys. Rev. D, 69, 103501
- Verde L., Peiris H. V., Spergel D. N., et al. 2003, ApJS, 148, 195
- Vielva P., Martínez-González E., Tucci M., 2006, MNRAS, 365, 891
- Wiener N., 1949, New York: Wiley
- Zaroubi S., 1995, in Maurogordato S., Balkowski C., Tao C., Tran Thanh van J., eds, Clustering in the Universe Wiener Reconstruction, SVD and ‘Optimal’ Functional Bases: Application for Redshift galaxy catalogs. p. 135
- Zaroubi S., Hoffman Y., Fisher K. B., Lahav O., 1995, ApJ, 449, 446
- Zhang P., 2006a, ApJ, 647, 55
- Zhang P., 2006b, Phys. Rev. D, 73, 123504